

First application of the massively-parallel Monte Carlo code ERO2.0 for plasma-wall interaction and 3D local impurity transport at JET ILW

J. Romazanov¹, D. Borodin¹, A. Kirschner¹, M. Firdaouss², A. Lasa³, D. Brömmel⁴,

B. Steinbusch⁴, P. Gibbon⁴, S. Brezinsek¹, Ch. Linsmeier¹ and JET Contributors*

EUROfusion Consortium, JET, Culham Science Centre, Abingdon, OX14 3DB, UK

¹ *Forschungszentrum Jülich GmbH, Institut für Energie- und Klimaforschung – Plasmaphysik,*

Partner of the Trilateral Euregio Cluster (TEC), 52425 Jülich, Germany

² *CEA, IRFM, F-13108 St Paul-Lez-Durance, France*

³ *Oak Ridge National Laboratory, Oak Ridge, TN 37831-6169, USA*

⁴ *Forschungszentrum Jülich GmbH, Institute for Advanced Simulation, Jülich Supercomputing*

Centre, 52425 Jülich, Germany

* *See Appendix of F. Romanelli et al., 25th IAEA Fusion Energy Conference (2014,*

St. Petersburg, Russia)

Introduction

Estimating erosion for plasma-facing components (PFCs) is one of the key issues for ITER. Effective sputter yields can be obtained experimentally e.g. by estimating flux ratios with S/XB ratios [1]. The interpretation of such experiments and extrapolation to ITER conditions is not straightforward, because the effective yields result from a complex interplay of plasma conditions, wall geometry and impurity transport. This makes modelling tools like the Monte-Carlo code ERO necessary. However, ERO was originally designed for simulation volumes of $\sim(10 \text{ cm})^3$, typically covering only a few adjacent wall tiles. This limitation is overcome by the new version ERO2.0. With a flexible 3D representation of wall geometries and plasma parameters, as well as increased performance due to massive parallelisation, ERO2.0 can simulate larger volumes with more PFC components. In this contribution, we re-visit recent ERO modelling from [1] for Beryllium (Be) erosion of the JET Inner-Wall Guard Limiter IWGL in octant 7X, tiles 6-8. The new code version allows the following improvements: 1) increased simulation volume in toroidal direction, 2) consideration of tiles from the neighboring IWGL limiters as particle sources, and 3) a more detailed model for magnetic shadowing of the wall. We focus on the effect of these improvements on Be self-sputtering.

Effect of an increased simulation volume

Fig. 1a shows the three simulation volumes used. In toroidal direction ϕ , the volume is centered around the limiter tip in 7X and has the extents $\Delta\phi = 11.25^\circ, 22.5^\circ, 33.75^\circ$. The two

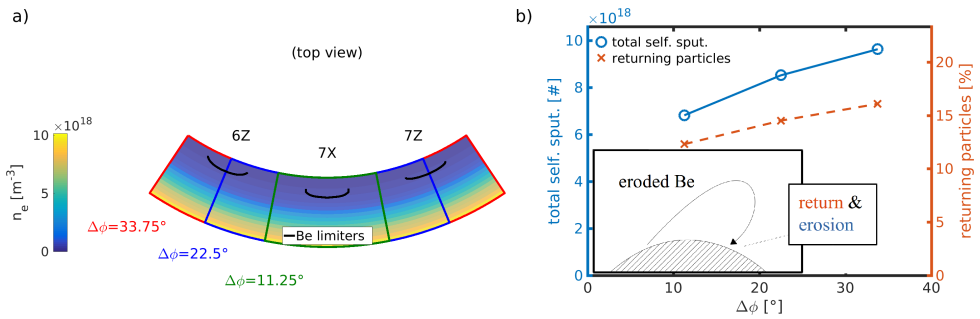


Figure 1: a) Top-view of the three simulation volumes used, varying in their toroidal extent $\Delta\phi$. The colormap indicates electron density n_e for JET discharge #81261. b) Self-sputtering integrated over all tiles (blue) and fraction of particles returning to the surface (red), compared for the three different volumes.

neighbor limiters in JET octants 6Z and 7Z are also shown, but are not considered yet in the simulation. The steps of 11.25° correspond to the approximate distance between the ridges of two neighboring poloidal limiters. Due to the fact that the two neighboring limiters are retracted radially, periodic boundary conditions in toroidal dimension seem inappropriate. Instead, the boundary condition is that particles which leave the volume boundaries are considered as lost. It should therefore be expected that the volume size should have an influence on Be impurity concentration in the plasma and self-sputtering.

Similar to [1], the constant plasma background was taken for JET discharge #81261 in the (R, Z) plane and rotated (assuming toroidal symmetry of the plasma) to get 3D maps as the one for n_e shown in Fig. 1a. The resulting Be self-sputtering patterns on the IWGL in 7X can be seen in Fig. 2h for $\Delta\phi = 33.75^\circ$. The patterns for the two other volume sizes are qualitatively very similar and therefore not shown. However, quantitatively we see an increase of self-sputtering with the volume size if we compare the respective values after integration over all surface cells (blue curve in Fig. 1b). The increase with volume size is almost linear, with the value for the largest volume being $\sim 40\%$ higher than for the smallest volume. This can be related to the fraction of particles returning to the limiter (red curve in Fig. 1b), which increased with volume, as some particles may reverse their velocity due to diffusive motion and return to the limiter surface. However, the slopes of the two curves are slightly different, which suggests that not only a higher fraction of particles is returning for larger simulation volumes, but also the incidence angle and energy distributions are changed.

Effect of neighboring limiters and improved shadowing model

In this section, we repeat the calculation for the largest volume of the previous section, but consider the Be transport coming from the neighboring limiters in octants 6Z and 7Z and its

effect on Be self-sputtering in 7X. The limiters in 6Z and 7Z are retracted in radial direction with respect to 7X by about 3.5 and 1.9 cm, respectively. Fig. 2a-c shows the patterns of the magnetic connection lengths L at the surface of tiles 6-8 in octants 6Z, 7X and 7Z, computed with the PFCFlux code [2]. One sees that the L -values of the retracted neighbor limiters in 6Z and 7Z are about an order of magnitude lower compared with 7X.

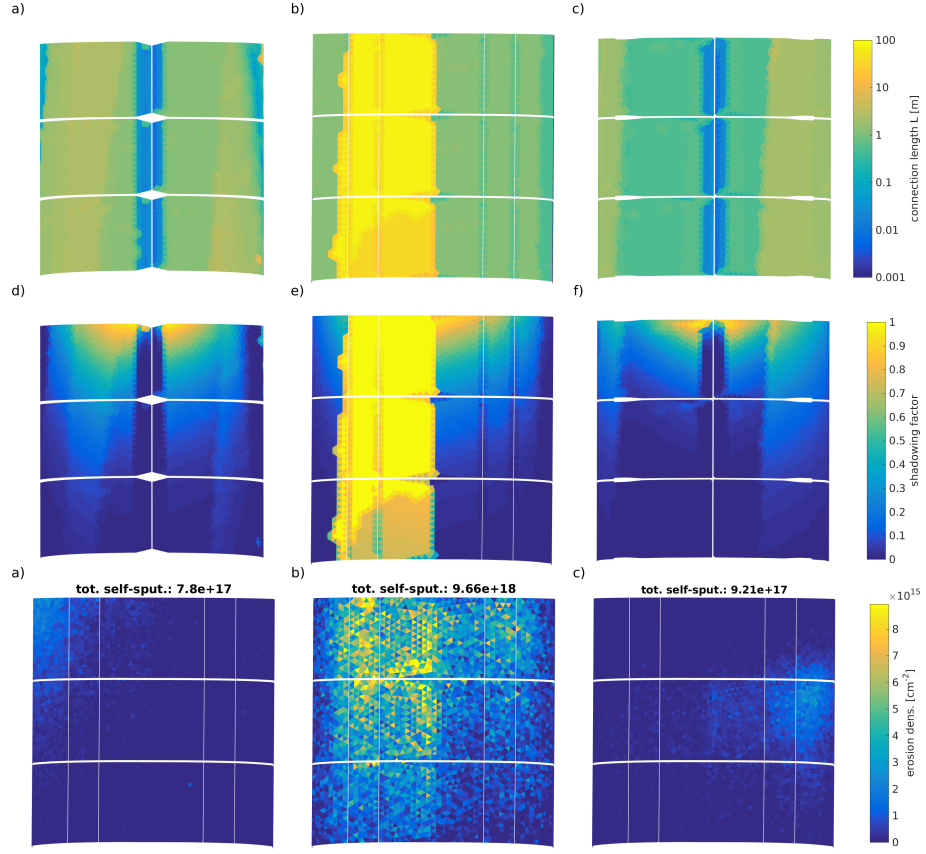


Figure 2: Top row: Connection lengths L (log-scale) computed with PFCFlux for octants a) 6Z, b) 7X and c) 7Z. Middle row: Shadowing computed with eq. (1) for octants d) 6Z, e) 7X and f) 7Z. Bottom row: Be self-sputtering patterns for octant 7X, created by Be particles eroded from octants g) 6Z, h) 7X and i) 7Z.

As the radial decay length of the electron density in the SOL scales with the connection length L , a shorter value of L will lead to a lower electron density and thus to lower erosion by the background plasma. Previously [1], this was treated phenomenologically in ERO by multiplying the erosion with a shadowing factor, which was set to 1 if L was above a certain threshold and 0 otherwise. This approach is too crude for the situation at hand, since the study is focused on transport of Be from neighboring limiters onto 7X, so that a very low threshold value would be required to get non-zero Be erosion of the neighbor limiters. Therefore, we make use of a more refined model recently presented in [3], in which the shadowing factor is computed

for an individual surface cell using an exponential approach

$$\text{shadowing} = \exp\left(-\frac{\Delta r}{\lambda_{\max}} \left(\sqrt{\frac{L_{\max}}{L_{\text{loc}}}} - 1\right)\right) \quad , \quad (1)$$

with index 'loc' meaning the local surface cell and 'max' the surface cell with the highest connection length L_{\max} at the limiter tip, and Δr the radial distance between the limiter tip and the local surface cell. Fig. 2d-e shows the shadowing patterns computed with eq. (1). After applying this shadowing model, the number of Be impurities created by background plasma sputtering in octants 6Z and 7Z is still lower than in 7X by roughly a factor of 10. Nevertheless, their contribution to Be self-sputtering in 7X is non-negligible. As can be seen in Fig. 2g-i, Be particles from neighboring limiters erode different locations in 7X. Also, the total contribution to self-sputtering in 7X from the neighbors amounts to $\sim 15\%$.

Conclusions

The new code ERO2.0 has been applied to investigate erosion of Beryllium tiles of JET's IWGL, with a special focus on self-sputtering. The volume was increased 3 times in toroidal direction, and tiles from the IWGLs in the two neighboring octants were added as Be impurity sources, utilizing the new code's increased performance due to massive parallelisation. The effect on self-sputtering (integrated over all surface cells) coming from these improvements was shown to be significant. The increased volume leads to a rise in self-sputtering by $\sim 41\%$ and the consideration of neighboring limiters contributes another $\sim 15\%$. Quantitative benchmarking with experimentally obtained sputter yields and spectroscopic measurements is ongoing, as well as an extended study with variation of plasma parameters.

Acknowledgements

This work has been carried out within the framework of the EUROfusion Consortium and has received funding from the Euratom research and training programme 2014-2018 under grant agreement No 633053. The views and opinions expressed herein do not necessarily reflect those of the European Commission. Computer time on JURECA was provided by the Jülich Supercomputing Centre under project VSR SLPP1.

References

- [1] D. Borodin et al, proceedings of 17th Int. Conference on Fusion Reactor Materials (ICFRM-17)
- [2] M. Firdaouss et al, J. Nucl. Mat. 438 (2013) S536-S539
- [3] A. Lasa et al, proceedings of 22nd International Conference on Plasma Surface Interactions in Controlled Fusion Devices (22nd PSI)